doi:10.2533/chimia.2022.852 Chimia 76 (2022) 852–859

Novel Insights on the Three-dimensional Shape of Microgels at Fluid Interfaces

Jacopo Vialetto*

Abstract: Mechanically soft colloids (microgels) adsorbed at the interface between two fluids offer superior advantages over hard counterparts for a variety of applications ranging from foams/emulsion stabilization to the assembly of two-dimensional (2D) materials. Particle deformability and compressibility impart additional responses to microgel-laden interfaces that can be controlled on-demand by varying single-particle properties (*e.g.* crosslinking content and polymer density profile) and/or external parameters (*e.g.* interfacial compression and tension, temperature, oil polarity). In order to understand how single-particle softness influences the resulting material properties, a detailed quantification of the microgel's 3D conformation when confined at the fluid interface is of utmost importance. This article describes how different methodologies can be used to visualize, and in some case quantify, the conformation of adsorbed microgels, putting particular emphasis on the multiple advantages offered by *in situ* atomic force microscopy imaging at the fluid interface. The influence of the internal particle architecture, as well as that of temperature, interfacial tension and solubility in the organic phase, will be discussed. Finally, some perspectives on how softness can be exploited to tune the structural and mechanical properties of microgel monolayers will be provided.

Keywords: Colloidal monolayers · Liquid interface · Mechanical properties · pNIPAM microgels · Volume phase transition temperature

Jacopo Vialetto studied Chemistry (BSc) at "La Sapienza" Univ. of Rome and Photochemistry and Molecular Materials (MSc) at the Univ. of Bologna (Italy). He received his PhD from the École Normale Supérieure (Paris, France) under the supervision of Prof. Damien Baigl in 2018. Currently, he is a Marie Curie research fellow at ETH Zurich (Switzerland) in the lab of Prof. Lucio Isa. His research interests include the study of the interactions of hard and soft colloidal particles with and at fluid interfaces. In particular, he focuses on developing strategies to tailor colloidal self-assembly into functional structures through internal (added chemicals or tailored synthesis protocols) and/or external (light) control.

1. Introduction

The interaction between colloidal particles and fluid interfaces is of relevance for a variety of materials and processes. Particle adsorption at air- and oil-water interfaces is responsible for the stabilization of foams and emulsions,[1,2] or the encapsulation, structuring and manipulation of liquids.[3,4] Particle assembly is exploited for the creation of model two-dimensional (2D) materials that are used for example in catalysis, optics, surface science.[5–8] Complex 2D structures can be advantageously assembled at the interface between two fluids, where the colloids display a plethora of interactions that often differ from the ones in bulk solution[9] and that guide the formation of assemblies unreachable in a single fluid phase.[10–12] On top of structural complexity, novel research directions now focus on developing responsive and reconfigurable devices[6,13] in which the particle assemblies respond to an external stimulus by changing their structure and properties.[14,15] For this scope, fluid interfaces offer significant advantages thanks to the high lateral mobility that the adsorbed colloids maintain, allowing one to tune the interparticle interactions and the resulting organization upon external stimulation.[11]

Currently, alongside hard, mechanically rigid colloids, soft micro- and nanoparticles are gaining much attention because of the responses to multiple stimuli that they offer once assembled at a fluid interface.[16,17] Softness in the building blocks imparts additional functionalities arising from the potential to tune the three-dimensional (3D) conformation of the adsorbed particles, which in turn affects the properties of the resulting monolayers.[18] Among various soft colloidal objects, microgels, *i.e.* solvent-swollen cross-linked polymer networks, are emerging as highly investigated models of soft particles. The relative ease in producing microgels with different internal architecture and polymer composition[19] makes them ideal candidates to investigate how these parameters affect the adsorption and organization of soft objects at fluid interfaces. Therefore, nowadays microgels are the subject of a large number of fundamental studies,[20–22] including their use to rationalize the behaviour of complex biological objects,[23,24] and are investigated for potential applications such as: on-demand destabilization of particle-stabilized foams and emulsions,[25] or surface patterning of ordered structures for lithography,[26] sensing[27] and optics.[28]

A first, significant difference between microgels and hard particles stems from the affinity of microgels for the fluid interface, which causes them to directly adsorb from the bulk of a suspension.[29,30] This is partially in contrast to rigid colloids that often experience an adsorption barrier that prevents contact with the liquid surface, whose energy depends on particle charge and hydrophobicity.[11]

The rich range of interactions acting among hard (spherical) particles at fluid interfaces is controlled by relatively few parameters, the most important of which are their surface charge and

*Correspondence: Dr. J. Vialetto, E-mail: jacopo.vialetto@mat.ethz.ch
Laboratory for Soft Materials and Interfaces, Department of Materials, ETH Zurich, Vladimir-Prelog-Weg 5, 8093 Zurich, Switzerland

contact angle (θ).[11,31,32] The contact angle is in particular the key quantity that indicates the relative protrusion of the colloid into the two fluids, and provides information on its affinity for the fluid surface. Therefore, a large number of techniques has been developed to measure θ.[33] The conformation of an adsorbed soft particle is, however, more complex. Softness causes the particle to deform and elongate on the interface plane under the action of interfacial tension. Moreover, differences in solubility of the polymer network in the two fluids give rise to asymmetric swelling. Consequently, reconfiguration and anisotropic deformation with respect to the bulk (spherical) shape make the definition of θ for a soft particle less meaningful. The anisotropic shape of an adsorbed microgel is also at the core of the multiple 2D structures that can be produced by interfacial assembly,[12,34] and of their complex responses upon interfacial compression.[35,36] This includes a rich phase behaviour as a function of packing fraction, with an extended tunability of the centre-to-centre distance between ordered particles,[26] and the existence of an isostructural phase transition.[35] Additionally, microgels' softness provides compliance in microgel-laden bubbles and drops, which greatly enhances their stability against coalescence when subjected to flows and processing.[37] Therefore, currently, a large number of studies has been focusing on tuning their interfacial conformation to gain control over the mechanical and structural properties of the resulting assemblies.[34,36,38]

A full 3D characterization of the shape of adsorbed soft particles is thus required to build a connection and gain predicting power over the polymeric structure in aqueous suspensions and their adsorption and desorption, dynamics and interactions at the interface. This article will describe how different methodologies allow visualizing and quantifying the 3D conformation of microgels adsorbed at a fluid interface, with particular emphasis on a novel approach we recently developed to reconstruct the 3D conformation of adsorbed microgels by means of *in situ* atomic force microscopy (AFM) imaging. I will then address how the microgel's internal polymer density profile, as well as various system parameters (*e.g.* temperature, interfacial tension, solubility in the two fluids), influence the conformation of adsorbed soft particles. Finally, I will discuss some examples that link the microgels' shape to their responses in materials (2D assemblies) and processes (emulsion destabilization).

2. 3D Conformation of a Soft Particle Adsorbed at a Fluid Interface

A large number of experimental techniques, often in combination with computer simulations, have been used to investigate the rearrangement of microgel particles upon adsorption at an air- or oil-water interface.[16] The results presented here focus on poly(N-isopropylacrylamide) (pNIPAM) microgels, which are commonly investigated soft particles; similar results can be expected for other polymer networks partially soluble in the water phase. Particularly advantageous *in situ* techniques are cryo scanning electron microscopy (cryo-SEM)[39] and freeze-fracture shadow-casting (FreSCa) cryo-SEM (Fig. 1a,b),[40,41] which provide high single-particle resolution and are applicable also to nanometre-sized objects. Cryo-SEM was used to visualize experimentally the flattened shape, also termed 'fried-egg' morphology that a microgel assumes at an oil-water interface. This conformation is characterized by a pronounced stretching of the particle into a polymer layer of decreasing thickness that spreads on the interface plane to minimize unfavourable fluid-fluid contacts, surrounding the core of the microgel that remains mostly in the water phase. Simulations supported these experimental findings, evidencing the anisotropic deswelling of the polymer network in the two fluids, and the presence of a thin polymer corona around the microgel core (Fig. 1c).

Nowadays, AFM has become a valuable tool for imaging colloidal-scale objects adsorbed at the interface between two fluids, allowing to capture in real-space and with fast acquisition times topographical images with exceptionally high lateral and vertical resolution. It has been used, for example, to investigate the microstructure of closely-packed nanoparticle monolayers, with diameters as small as 13 nm,[42,43] or to acquire spatial and mechanical information on polymeric films formed at an oil-water interface.[44,45] Time-resolved imaging allows capturing adsorption events of a nanoparticle to a populated fluid interface, and rearrangements of the neighbouring colloids.[46]

Recently, we extended the applicability of AFM imaging at an oil-water interface to characterize *in situ* the conformation of an adsorbed microgel.[47] The use of two experimental setups with the AFM tip immersed either in the oil or water phase allowed us to capture images from both fluids and consequently reconstruct the entire 3D shape of an adsorbed particle in (virtually) the same experimental conditions. It is noteworthy to emphasize that *in situ* AFM imaging offers several advantages over other techniques used to visualize the conformation of adsorbed microgels. In particular, it can be performed in solution under ambient conditions, without the need for fast freezing (as required, for example, for cryo-SEM) or drying of the samples, therefore limiting possible perturbations and modifications of the soft polymer network. Additionally, it allows to quantify the 3D topography of the particles in real-time as a function of a variety of experimental conditions; *e.g.* different fluids, solution temperature and monolayer density.

Fig. 1d shows the 3D reconstruction of the shape of a single microgel at the hexadecane-water interface, while height images of ordered microgel monolayers captured from the oil and water side are reported in Fig. 1e,f. Imaging from either side of the interface provides a precise quantification of the anisotropic deformation of the adsorbed soft particle. The microgel is significantly stretched out, reaching an interfacial diameter that is almost twice the hydrodynamic size in the bulk aqueous phase. Progressive flattening from the centre to the edge of the particle is evidenced in both fluids, albeit to a different extent. The highly anisotropic swelling in the two liquids stems from differences in the solubility of the polymer network. The polymer chains in the apolar phase are in a bad solvent and are collapsed onto the microgel core. Consequently, the particle only barely protrudes out into the oil phase, leaving only a very thin polymer layer up to the particle periphery. In contrast, water at room temperature is a good solvent for pNIPAM and the polymer network is fully hydrated on the aqueous side of the interface. In the case of microgels in contact, the pronounced swelling on the water side causes the polymer networks to overlap, forming a large contact region below the interface with possible compression and interpenetration of the outer part of the microgels. Such an overlap precludes the visualization of the full microgel height profile from the water side in closely packed monolayers, as the AFM tip cannot reach the bare fluid interface and the height information is only relative to the contact region between neighbouring particles (see the height colour-bar in Fig. 1f). From the oil side, instead, microgels only sterically interact with their polymer chains spread on the fluid interface plane. While these chains are only barely visible in height images, they can be fully captured by monitoring the adhesion between the AFM tip and the adsorbed microgels.[47]

Complementary approaches such as ellipsometry[48] and neutron reflectivity[49,50] also provide information on the different thicknesses of adsorbed microgel layers in the fluid phases. For both nanogels[49] and microgels,[50] fitting of neutron reflectivity curves with models that include multiple layers perpendicular to the interface plane indicate that the microgels are significantly deformed and flattened at the fluid interface. The protrusion height into the water phase is much greater with respect to that into the upper fluid (air in these cases), and shows a decrease in the polymer volume fraction as a function of distance from the interface that is consistent with the network swelling in the aqueous phase.

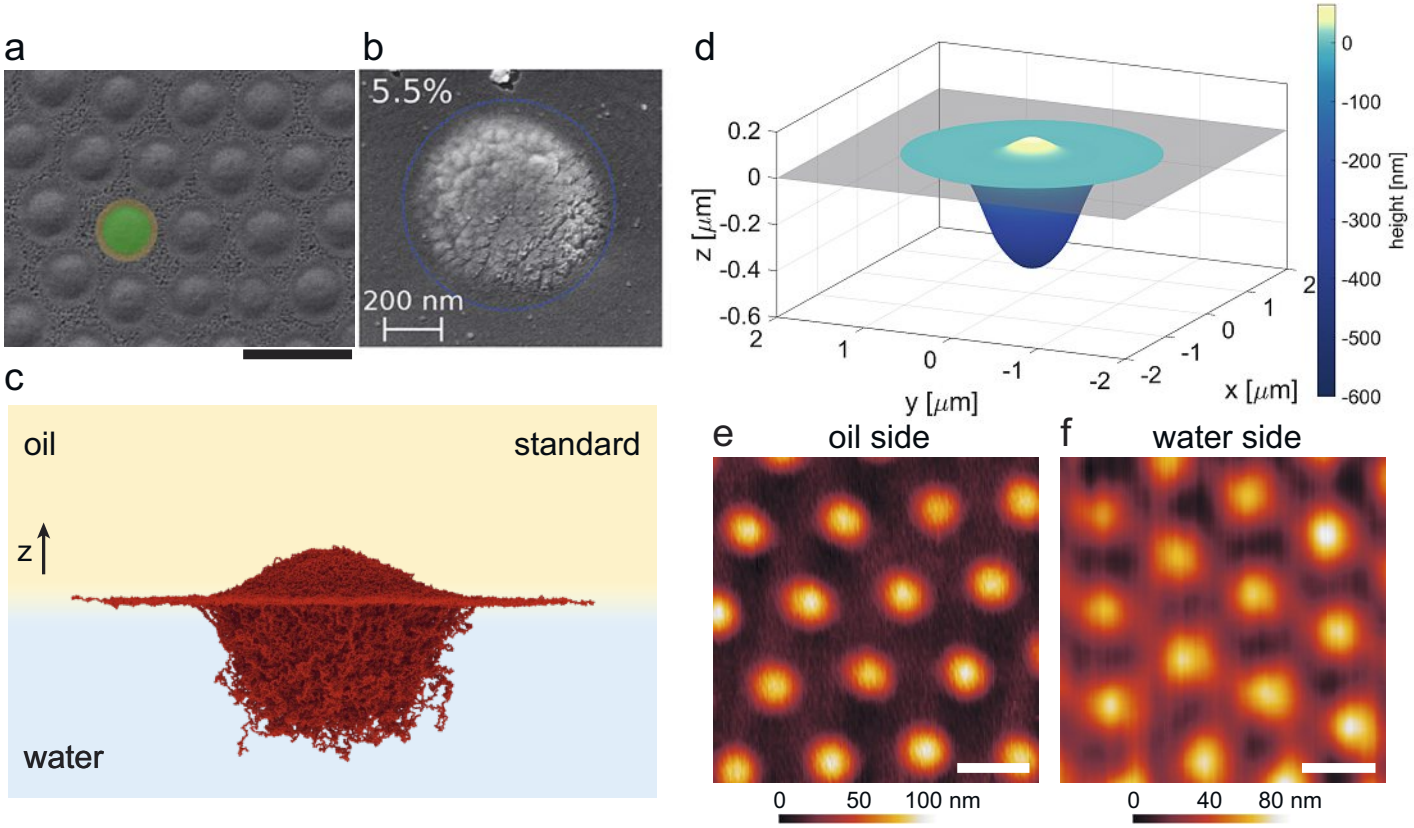

Fig. 1. Conformation of a pNIPAM microgel adsorbed at a fluid interface. a) FreSCa cryo-SEM image of microgels at a n-heptane-water interface imaged from the oil side. Scale bar: 1 μm. Adapted with permission from ref. [40]. Copyright 2012 American Chemical Society. b) FreSCa cryo-SEM image of the protrusion into the oil phase of a microgel with 5.5 mol % crosslinker. The blue circle corresponds to the average diameter. Adapted with permission from ref. [41]. Copyright 2019 American Chemical Society. c) Simulation snapshot of a microgel at the oil-water interface. Adapted with permission from ref. [36]. Copyright 2021 American Chemical Society. d) Reconstructed 3D profile from *in situ* AFM images of a microgel with 5 mol % crosslinker at the hexadecane-water interface: the grey rectangle indicates the interface plane, negative heights the protrusion into the water phase. e,f) AFM height images of microgels imaged from the hexadecane (e) and water (f) side. Scale bar: 1 μm. d-f) Adapted from ref. [47].

Optical and confocal microscopy have also been used to investigate microgels at fluid interfaces,[39,51,52] however, they are often limited to micrometre-sized particles, require fluorescent markers, and typically do not ensure high enough spatial resolution perpendicular to the interface. On the other hand, they provide information on the in-plane size of the particles by looking at the centre-to-centre distance between neighbours.

An alternative approach to investigate the conformation of microgels adsorbed at fluid interfaces consists of transferring them onto a solid substrate for *ex situ* AFM or SEM imaging.[36,38] The AFM profiles obtained by this method closely mirror the polymer density distributions of the adsorbed microgels projected onto the plane defined by the fluid interface, and this technique is frequently used as a rapid and straightforward way to capture the anisotropic conformation and in-plane stretching of the particles. However, it can only resolve a 2D projection of the polymer distribution across the interface for a particle in a dry or re-hydrated state, and does not give direct access to its 3D shape at the interface. Additionally, it might be affected by specific particle-substrate interactions altering the particle conformation.[53] Particle-substrate interactions become particularly relevant in the case of hard-core soft-shell particles.[54] For large core dimensions with respect to the shell thickness, geometrical effects cause a systematic decrease of the measured total size after transferring since the soft shell has to deform after coming into contact with the substrate to accommodate the hard core, making such measurements unreliable for a precise quantification of the particle conformation at the fluid interface.

The extent of stretching on the interface plane, as well as that of swelling in the water phase, are linked to the internal elasticity of the microgels. At the same time, external parameters such as the interfacial tension value, the relative solubility of the polymer network in the two fluids used, and the solution temperature in case of thermo-responsive polymers, influence the conformation of the adsorbed particles. All these parameters will be discussed in the following two sections.

2.1 *Influence of the Internal Polymer Density Profile*

The anisotropic morphology of an adsorbed microgel has been attributed not only to the flattening on the interface plane under the action of interfacial tension and to the different solubility in the fluids, but also to the conformation of the polymer network in the bulk aqueous phase. 'Standard' pNIPAM microgels are commonly obtained by free-radical precipitation polymerization in the presence of a crosslinker.[19] Due to the faster reaction rate of most crosslinkers with respect to NIPAM,[55] the microgels develop a morphology characterized by a more cross-linked (denser) core and a less cross-linked corona. In addition, uncross-linked chain ends form an external 'hairy' surface.[56] The presence of such a gradient in crosslinking density is thought to contribute significantly to the rearrangement of the polymer network at the interface, leading to the typically observed 'fried-egg' morphology. A precise tuning of the microgels internal architecture at the synthesis level affects the elasticity and deformability of the particles.[18] Consequently, several works investigated whether this would also control the extent of deformation and swelling at the fluid interface.

The most straightforward way to modify the network elasticity is to vary the crosslinker content. Particles produced with a lower amount of crosslinker show an increased swelling in bulk water,[57] as well as a decrease in their elastic modulus.[58] At fluid

interfaces, this results in a more pronounced in-plane flattening and a greater cross-sectional area, as evidenced both by *in situ* and *ex situ* techniques by calculating the stretching ratio with respect to their bulk size.[38,41] At the same time, the polymer protrusion in both the upper and the lower fluids decreases.[47,49] Despite the more pronounced stretching, a 'fried-egg' structure is always observed when a crosslinker is added during synthesis,[59] as a consequence of the gradient in stiffness in the polymer network from the core to the edge of the particle. More refined synthesis protocols allow for carefully tuning the internal polymer density profile in order to affect the final conformation of adsorbed microgels. For example, a two-step polymerization reaction can be used to produce 'inverse' particles that are characterized by an ultra-low crosslinked core and a crosslinked shell.[47] *In situ* AFM imaging at the fluid interface (Fig. 2b) revealed that these microgels flatten out on the oil side, assuming an almost constant thickness up to the visible particle periphery. The low amount of crosslinks in the core allows such particles to deform more than 'standard' microgels at the interface in order to maximize the amount of adsorbed polymer, while remaining significantly swollen on the water side.

Scotti *et al.*[60] and Bochenek *et al.*[50] investigated microgels obtained *via* self-polymerization of NIPAM triggered by persulfate-initiated reactions in the absence of a crosslinking agent, so-called ultra-low crosslinked (ULC) microgels. Such particles are formed by chain-transfer reactions that induce self-crosslinking between pNIPAM chains, have a larger mesh size and possess significantly increased deformability with respect to 'standard' ones. AFM imaging after adsorption at the oil-water interface and transfer onto a solid substrate showed that ULC microgels strongly flatten into disks, with a stretching ratio calculated with respect to their bulk size that is significantly higher than regularly crosslinked microgels.[60] *In situ* neutron reflectivity data revealed that, analogous to the 'inverse' microgels presented before, ULC microgels barely protrude into the air phase.[50] The majority of the polymer can be found on the interface plane, while the extension in the water phase is similar to that of 'standard' microgels, albeit with a much lower polymer density. Simulations also confirmed that ULC microgels significantly stretch on the interface plane.

In order to assess the interplay between internal microgel architecture and conformation at the interface, we investigated core-shell microgels made of a soft pNIPAM core with a cleavable crosslinker that can be chemically removed in a controlled fashion.[36] This strategy allowed us to obtain a series of particles ranging from analogues of 'standard' microgels to completely hollow ones after total core removal. Simulation snapshots of the initial and final states are reported in Fig. 2d. The conformation at the

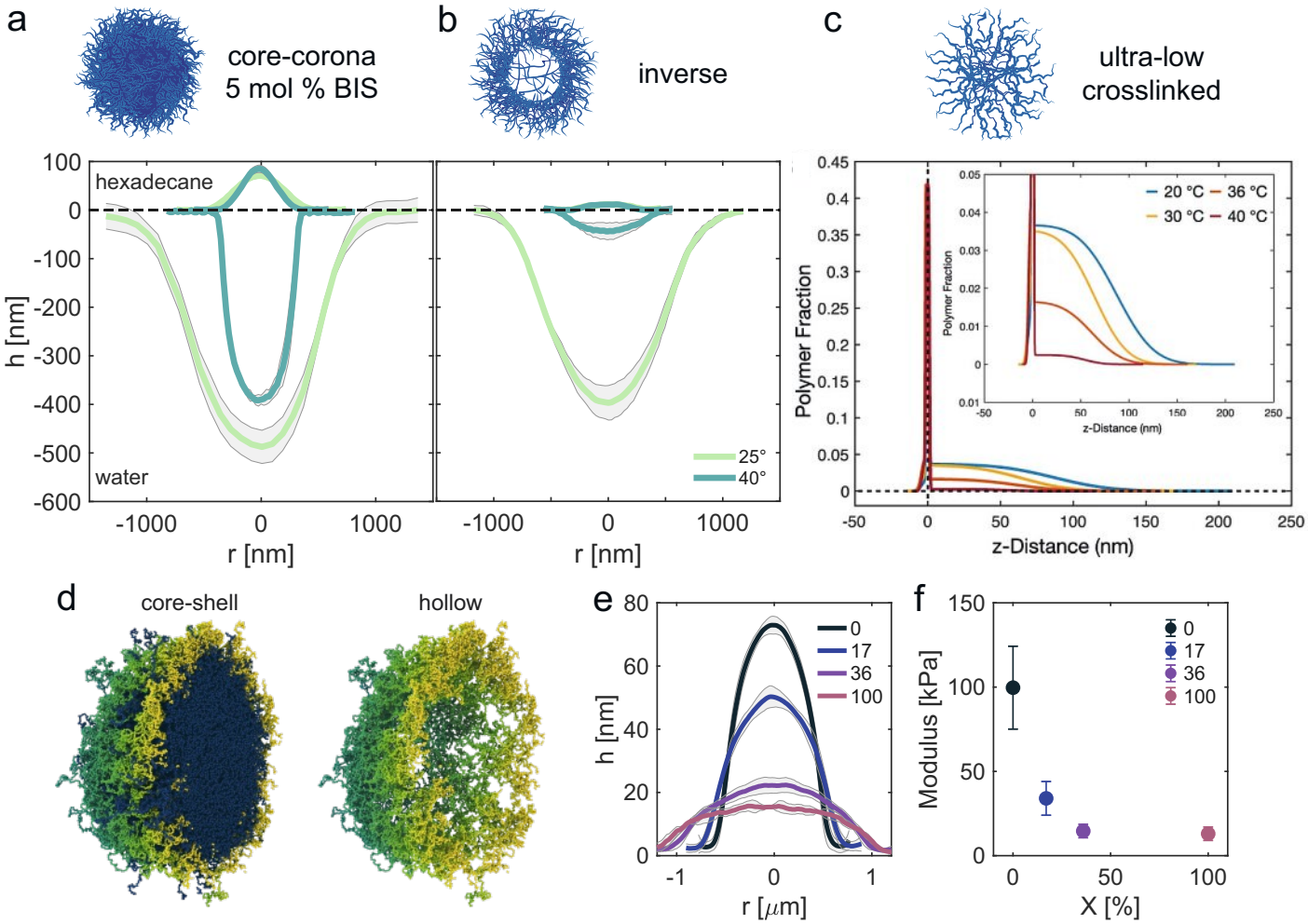

Fig. 2. Influence of the internal polymer density profile on the conformation of microgels at fluid interfaces. a-b) Sketch of a 'standard' (a) and an 'inverse' (b) microgel and corresponding height profiles from *in situ* AFM images at the hexadecane-water interface (water at negative h values) at 25 °C and 40 °C. Adapted from ref. [47]. c) Sketch of an ultra-low crosslinked microgel and polymer fraction across the air-water interface (water at positive z values) as a function of the solution temperature, as obtained by neutron reflectivity. Adapted from ref. [50]. Copyright 2022 Springer Nature. d) Simulations of a core-shell and a hollow microgel in bulk. e) Dry height profiles of microgels after deposition onto a silicon wafer from the hexane-water interface, as a function of different % of core removal (0 % = core-shell; 100 % = hollow). f) Microgels Young's modulus obtained from AFM nanoindentation measurements as a function of % of core removal. d-f) Adapted with permission from ref. [36]. Copyright 2021 American Chemical Society.

interface was analysed *via* the transfer of the adsorbed particles from the oil-water interface onto a silicon wafer, together with comparisons with simulations. This revealed how progressive removal of the crosslinked core induces flattening of the microgels and an increase in the extension on the interface plane. A decrease up to three times of the initial height was obtained already for only 40% of core removal (Fig. 2e), suggesting that, for this particle architecture, a critical number of crosslinks in the internal polymer network are cleaved and the particle stiffness rapidly decreases. A quantification of the resulting particle stiffness was obtained by AFM nanoindentation experiments, which show a significant reduction of the particles' Young's modulus in conjunction with the change in morphology (Fig. 2f).

Finally, FreSCa was used to investigate the conformation of adsorbed silica-pNIPAM hard-core soft-shell particles as a function of the shell thickness.[61] These particles assume the common 'fried-egg' morphology with a significant stretching of the pNIPAM network on the interface plane. The absence of a shadow around the particles after oblique metal coating in FreSCa indicates that the particles only slightly protrude out the water phase, with a contact angle that remains below 30° and the silica core that remains mostly, or totally, submerged into the water phase. However, the rigid core precludes the shell to fully relax the deformation due to interfacial confinement. As a consequence, the shell induces a deformation of the surrounding fluid interface and the appearance of attractive capillary interactions. The extent of the shell deformation at the interface was found to be the same irrespective of the core-to-shell ratio.

2.2 *External Parameters: Temperature, Interfacial Tension and Polymer Solubility*

pNIPAM particles, or microgels made with other thermoresponsive polymers, undergo a volume phase transition as a function of the solution temperature (VPTT) due to a solubility change from good to bad solvent conditions upon temperature increase, which causes a reversible switch from swollen to collapsed particles. This response is maintained at the fluid interface, albeit with some relevant differences. Above the VPTT, corresponding to T ~32 °C for pNIPAM in water, microgels are stretched out on the interface plane and assume a highly non-spherical shape irrespective of their internal architecture (see Fig. 2a–c for 'standard', 'inverse'[47] and ULC[50] conformations). Oil and air are always bad solvents for pNIPAM and the profiles on the upper side remain essentially unaltered, with collapsed polymer chains onto the microgel core. Deswelling can instead be observed in the water phase. Quantification of the interfacial swelling ratio of 'standard' microgels indicates that while the particles maintain thermal responsiveness, the degree of deswelling with respect to isotropic shrinkage in suspension is restrained by the interfacial confinement.[47,50] Similar results have been evidenced also by using other techniques: *ex situ* AFM imaging revealed the presence of a core-corona structure also above the VPTT,[62] while ellipsometry[48,63] was used to quantify the decrease of the out-of-plane extension of the microgels into the water phase.

An appropriate choice of the internal microgel architecture allows to modulate the extent of deswelling in the aqueous phase. Both 'inverse' (Fig. 2b)[47] and ULC (Fig. 2c)[50] microgels behave differently to 'standard' ones, and undergo a pronounced conformational change in water above the VPTT. The presence of a highly swollen and loosely crosslinked core below the VPTT induces an almost complete collapse of the polymer network upon temperature increase, leaving only a thin polymer layer on the fluid interface. Interestingly, these results suggest that particles with a very soft core might perform better as switchable stabilizers for the production of temperature-sensitive emulsions.

Two other parameters play a fundamental role in dictating the conformation of adsorbed microgels. First, interfacial tension (γ) is responsible for pulling the adsorbed polymer radially outward, maximizing the area of the interface covered by the particles at the expense of microgel deformation. Most studies addressing microgel conformation, assembly and interfacial properties are typically focused on air-water or alkane-water interfaces, which are characterized by high γ values, ranging from 72 to ~50 mN/m. Additionally, as already discussed, in both cases pNIPAM is essentially insoluble in the top phase. This imparts similar conformations to the adsorbed microgels that, presumably, stretch out up to the maximal extent allowed by their internal elasticity. Consequently, the adsorbed monolayers display analogous structural and mechanical behaviours upon interfacial compression.[62,64]

The interface can be engineered to control the shape of adsorbed microgels by using fluids with a significantly lower γ value. Recently, we investigated conformational changes in microgels adsorbed at the interface between hexane (γ = 50.4 mN/m), toluene (γ = 36.3 mN/m) or methyl tert-butyl ether (MTBE, γ = 9.8 mN/m) and water, by *ex situ* AFM imaging (Fig. 3a).[65] In all cases, the microgels assume a core-corona profile; however, in the lowest γ case, the maximum microgel height is increased while the in-plane deformation is reduced. Both variations indicate that the internal elasticity of the crosslinked cores is able to counterbalance the deformation imposed by interfacial tension, resulting in a lower in-plane stretching of the microgels at the MTBE-water interface. Conversely, the extent of the outer corona did not change; in all cases, the uncrosslinked polymer chain ends could expand unconstrained on the fluid surface to the same extent. Similar results were obtained for microgels with different crosslinking densities, with the exact lateral stretching and height values being dependent on the network stiffness. It is important to note that pNIPAM is essentially insoluble in these three solvents. We could therefore attribute changes in their conformation mainly to the γ value.

The solubility of the polymer network in the top phase also plays a crucial role. It is however difficult to decouple the effect of γ and anisotropic swelling as interfaces between water and oils in which pNIPAM is soluble, such as fatty alcohols, also have γ ~ 10 mN/m. Destribats *et al*.[66] evidenced, by using both confocal microscopy and cryo-SEM, that the centre-to-centre distance between microgels adsorbed at the octanol-water interface is close to the bulk hydrodynamic diameter of the particles at 25 °C. This observation corroborates the conclusion that, in the case of low γ values, the particles are only weakly deformed within the interface plane. *In situ* AFM imaging at the 1-decanol-water interface allowed for a quantification of the out-of-plane extension of the adsorbed microgels.[47] Both images of a monolayer from the 1-decanol side (Fig. 3b) and the reconstructed microgel shape (Fig. 3c) show how the polymer network undergoes swelling of a similar extent in the two solvents, assuming an almost symmetrical profile across the interface. Moreover, the reduced value of the interfacial tension leads to a significantly lower deformation within the interface plane with respect to the same particles at the hexadecane-water interface (Fig. 1d). Notably, the deviation from a rounded shape is concentrated in proximity of the interface plane, similar to prediction for neutrally wetting soft spheres.[67] Swelling in the organic phase implies that the standard 'fried-egg' morphology is no longer applicable. Additionally, in the case of neighbouring particles, the polymer network now overlaps and possibly interpenetrates on both sides of the interface.

It is interesting to note that for hard particles an increased protrusion into the top phase indicates a variation in their hydrophilicity/hydrophobicity, contact angle and affinity with respect to the interface. In contrast, for soft particles such a conclusion cannot be drawn due to the complex dependence of the particle shape on γ, solubility in the solvents, and internal elasticity. Indeed, microgels show high affinity, and are very good stabilizers, towards

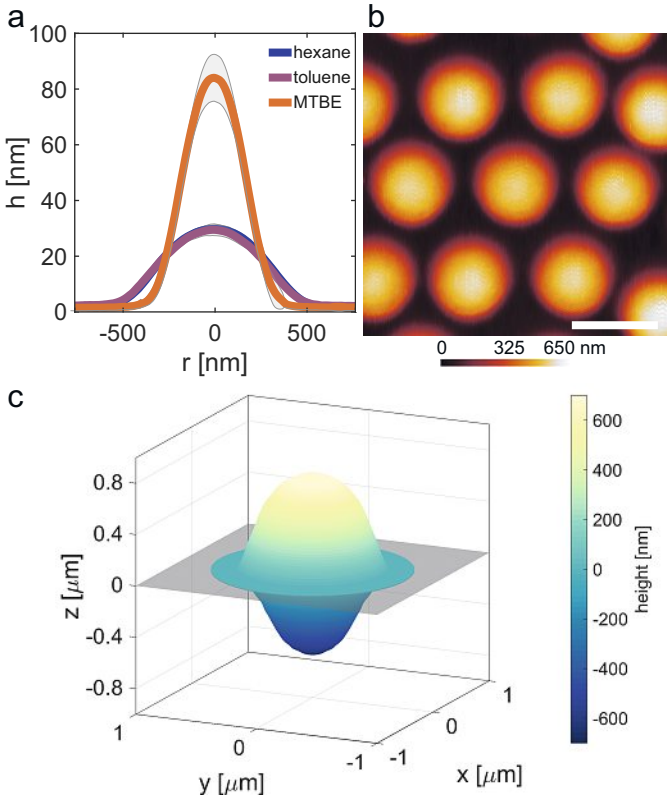

Fig. 3. Microgels conformation at different oil-water interfaces. a) Dry height profiles of microgels after deposition onto a silicon wafer from different oil-water interfaces. Adapted with permission from ref. [65]. Copyright 2022 Elsevier. b) *In situ* AFM image of microgels at the 1-decanol-water interface, imaged from the 1-decanol side. Scale bar: 1 μm. c) Reconstructed 3D profile from *in situ* AFM images of a microgel at the 1-decanol-water interface: the grey rectangle indicates the interface plane, negative heights the protrusion into the water phase. b-c) Adapted from ref. [47].

interfaces formed between water and either apolar or polar oils. However, while they stabilize oil-in-water emulsions in the former case, water-in-oil emulsions are obtained in the presence of polar oils.[66]

3. Tunable 2D Assemblies

The conformation that adsorbed microgels assume at a fluid interface has direct implications on their self-assembly by governing both the structural organization and the mechanical properties of the monolayers when subjected to compression and/or other external stimuli (*e.g.* temperature variations). This has a significant impact in a range of applications and processes in which microgel-laden interfaces are involved, from the stabilizations of foams and emulsions against coalescence and rupture, to the assembly of long-range ordered structures for particle-based lithography. Far from providing a comprehensive review on the subject, which can be found for example in refs [16] and [18], I here provide some examples on the link between single-particle morphology at the interface and the monolayer properties.

A direct consequence of the 'fried-egg' morphology of 'standard' microgels is that they display, when adsorbed on flat fluid interfaces, a solid-solid phase transition upon monolayer compression.[35] Starting from a sparse microgel monolayer, continuous interface compression first causes an increase in surface pressure when microgels come into contact through their coronae and start compressing isotropically up to a certain deformation ratio. In this regime, only deformation of the outer coronae is presumed to contribute to the increase in the monolayer surface pressure, while the more crosslinked core remain essentially unaltered. Further compression induces, in the majority of cases, failure of some of the coronae and the nucleation of a cluster phase of particles in core-core contacts, up to complete compression of all the coronae and the formation of a hexagonal closely packed phase.

The absence of an isostructural transition has been reported in the case of nanogels, with a diameter of at most few hundred nanometres,[68] for microgels with a low crosslinking density,[38,69] or with a hollow structure.[36] In the first case, upon increasing compression the microgels assemble in a disordered phase due to an amplified polydispersity at the interface resulting from variability in their internal structure. In the other two cases, a similar continuous decrease of the lattice constant in ordered monolayers was observed, but it was ascribed to a different reconfiguration of the compressible particles. Simulations predict that loosely crosslinked microgels would compact in a continuous manner due to the presence of a single characteristic internal length scale, which gives rise to a repulsion energy that increases non-linearly (with a convex shape) as a function of the decreasing interparticle distance.[38] Hollow microgels instead present two characteristic internal length scales and do not undergo a continuous compression upon increasing the interfacial pressure.[36] At low compression, the monolayer response was found to be similar to that of 'standard' core-corona microgels; both experiments and simulations showed that, in this regime, microgels only compress their outer polymer chains, deforming in a limited manner. Conversely, at high compression, the absence of the core enables the hollow particles to expand out of the interface plane to accommodate the increasing pressure maintaining an overall ordered structure.

Interestingly, hard-core soft-shell microgels were found to transition from a non-close-packed hexagonal phase to an assembly into a chain network. The occurrence of anisotropic interactions between isotropic building blocks is attributed to the presence of an energy minimum at intermediate compressions in which the corona surrounding the cores fully compress along the chain direction, while remaining stretched in the direction perpendicular to it.[38,70] A qualitatively different response was instead obtained for ultra-low cross-linked microgels that, at intermediate compression, behave as flexible polymers and distribute into a uniform polymer film covering the fluid interface, where the single microgels become indistinguishable. The shape of the microgels is recovered at high compression, when they assemble into a disordered structure due to their size and mechanical polydispersity.[60]

Several works investigated the effect of external parameters on the stability and structural organization of microgel monolayers. For example, increasing the solution temperature above the VPTT of pNIPAM was found to alter the monolayer response to compression in correspondence to the isostructural phase transition.[48] At low compression, the corona-corona contacts between microgels are not modified by the temperature increase as the in-plane stretching of the particles is similar. Instead, deswelling of the polymer network in the water phase at high temperature increases the average polymer density at the interface, precludes further compression of the core, and the microgels become incompressible once the isostructural transition is completed. The interfacial tension value also plays a role in controlling the response of microgels monolayers upon compression. As for the single particle conformation, between air-water and alkane-water interfaces the microgel assemblies have essentially a similar 2D phase behaviour.[64] Instead, at interfaces characterized by a much lower γ value (MTBE-water, γ = 9.8 mN/m) while qualitatively similar hexagonal structures are obtained, the assemblies display different mechanical responses.[65] A lower γ value makes the microgels more deformable and facilitates the compression of the coronae, shifting the onset of the isostructural phase transition to larger interparticle distances. Upon further interfacial compression, the cores directly enter into core-core contacts due to a

complete collapse of the polymer composing the coronae, which presumably partially desorb from the interface.

4. Conclusions and Perspectives

This paper briefly reviews some of the existing techniques used to assess the shape of soft microgels at a fluid interface, and provides some examples to address how this affects their 2D assembly. Their intrinsic softness translates into a pronounced deformation and shape-change with respect to the same particles in bulk aqueous conditions. Recent findings showed how a rational choice of the synthetic routes used to produce microgels having different internal architectures offers a powerful tool to modulate and control the conformational rearrangements following adsorption at the interface. Additionally, external parameters such as temperature, interfacial tension value and polymer solubility in the organic phase, provide an orthogonal control over the polymer network conformation. A precise quantification of the profile of both single microgels and microgels in contact is expected to improve significantly our understanding on the interaction between soft particles, of relevance for gaining a more advanced control over emulsion stabilization and microstructural assembly in ordered monolayers.

For example, visualization of the particle conformation across the VPTT can help rationalize the mechanism behind destabilization of microgel-laden emulsion drops by temperature increase[62,63,71] by allowing to quantify the extent of collapse of the polymer network in the aqueous phase. To this regard, novel findings obtained by *in situ* AFM imaging[47] and neutron reflectivity[50] revealed how the internal microgel architecture controls the particle volumetric swelling in water, suggesting that particles with a more loosely crosslinked core will perform as better stabilizers for the production of temperature-sensitive emulsions. Similarly, investigation on the microgel swelling as a function of the solubility of the network in the organic phase might provide additional information to predict which phase will be the dispersed one during emulsion formation.[66] Indeed, the exact microgel conformation was found to be dependent on the oil phase properties. For adequately low interfacial tension values ($\gamma \sim 10$ mN/m), the internal elasticity of 'standard' microgels is sufficient to preclude a full stretching of the polymer layer, decreasing the particle cross-sectional area on the interface plane. Solubility of the network in the organic phase is instead responsible for a significant swelling of the microgel also in the top phase and causes a marked departure from the commonly observed 'fried-egg' morphology.

Very recently, the group of Richtering developed synthesis methods to produce anisotropic, ellipsoidal microgels with either a hard or a hollow core and a soft polymeric shell.[72] Such a remarkable control over the internal architecture and shape of soft particles will improve our ability to program the conformation of adsorbed microgels, and predict how more complex biological objects (*e.g.* proteins, cells and viruses) behave when confined at fluid interfaces.[73] A complete 3D characterization *in situ* of the conformation of adsorbed anisotropic microgels will surely contribute in visualizing and understanding their interfacial rearrangement and behaviour in 2D assemblies.

More in general, a detailed *in situ* visualization of their packing and deformation from both sides of the fluid interface is expected to provide novel findings to help in rationalizing and predicting their phase behaviour. Indeed, this might disclose *in situ* rearrangements of neighbouring microgels subjected to compression as a function of their internal polymer network, and at different compression stages. In combination with simulations, this will allow assessing the different contributions to the total interaction potential stemming from the repulsive interaction between overlapping networks at increasing compression and the extent of the internal length scales at play at each compression stage.

Acknowledgements

I would like to acknowledge Prof. Lucio Isa for the multiple insightful discussions on this topic and for critical inputs on the manuscript. I acknowledge funding from the European Union's Horizon 2020 research and innovation programme under the Marie Skłodowska Curie grant agreement 888076.

Received: August 31, 2022

[1] B. P. Binks, R. Murakami, *Nat. Mater.* **2006**, *5*, 865, https://doi.org/10.1038/nmat1757.
[2] P. J. Beltramo, M. Gupta, A. Alicke, I. Liascukiene, D. Z. Gunes, C. N. Baroud, J. Vermant, *Proc. Natl. Acad. Sci.* **2017**, *114*, 10373, https://doi.org/10.1073/pnas.1705181114.
[3] G. Di Vitantonio, T. Wang, M. F. Haase, K. J. Stebe, D. Lee, *ACS Nano* **2019**, *13*, 26, https://doi.org/10.1021/acsnano.8b05718.
[4] M. Anyfantakis, V. S. R. Jampani, R. Kizhakidathazhath, B. P. Binks, J. P. F. Lagerwall, *Angew. Chemie Int. Ed.* **2020**, *59*, 19260, https://doi.org/10.1002/anie.202008210.
[5] P.-P. Fang, S. Chen, H. Deng, M. D. Scanlon, F. Gumy, H. J. Lee, D. Momotenko, V. Amstutz, F. Cortés-Salazar, C. M. Pereira, Z. Yang, H. H. Girault, *ACS Nano* **2013**, *7*, 9241, https://doi.org/10.1021/nn403879g.
[6] Y. Montelongo, D. Sikdar, Y. Ma, A. J. S. McIntosh, L. Velleman, A. R. Kucernak, J. B. Edel, A. A. Kornyshev, *Nat. Mater.* **2017**, *16*, 1127, https://doi.org/10.1038/nmat4969.
[7] N. Vogel, R. A. Belisle, B. Hatton, T.-S. Wong, J. Aizenberg, *Nat. Commun.* **2013**, *4*, 2176, https://doi.org/10.1038/ncomms3176.
[8] J. Vialetto, S. Rudiuk, M. Morel, D. Baigl, *Nanoscale* **2020**, *12*, 6279, https://doi.org/.1039/C9NR10965J.
[9] F. Bresme, M. Oettel, *J. Phys. Condens. Matter* **2007**, *19*, 413101, https://doi.org/10.1088/0953-8984/19/41/413101.
[10] N. Vogel, M. Retsch, C.-A. Fustin, A. del Campo, U. Jonas, *Chem. Rev.* **2015**, *115*, 6265, https://doi.org/10.1021/cr400081d.
[11] J. Vialetto, M. Anyfantakis, *Langmuir* **2021**, *37*, 9302, https://doi.org/10.1021/acs.langmuir.1c01029.
[12] F. Grillo, M. A. Fernandez-Rodriguez, M.-N. Antonopoulou, D. Gerber, L. Isa, *Nature* **2020**, *582*, 219, https://doi.org/10.1038/s41586-020-2341-6.
[13] S. Srivastava, D. Nykypanchuk, M. Fukuto, O. Gang, A*CS Nano* **2014**, *8*, 9857, https://doi.org/10.1021/nn5042416.
[14] J. Vialetto, M. Anyfantakis, S. Rudiuk, M. Morel, D. Baigl, *Angew. Chemie Int. Ed.* **2019**, *58*, 9145, https://doi.org/10.1002/anie.201904093.
[15] J. Vialetto, S. Rudiuk, M. Morel, D. Baigl, *J. Am. Chem. Soc.* **2021**, *143*, 11535, https://doi.org/10.1021/jacs.1c04220.
[16] M. Rey, M. A. Fernandez-Rodriguez, M. Karg, L. Isa, N. Vogel, *Acc. Chem. Res.* **2020**, *53*, 414, https://doi.org/10.1021/acs.accounts.9b00528.
[17] E. Guzmán, A. Maestro, *Polymers (Basel)* **2022**, *14*, 1133, https://doi.org/10.3390/polym14061133.
[18] A. Scotti, M. F. Schulte, C. G. Lopez, J. J. Crassous, S. Bochenek, W. Richtering, *Chem. Rev.* **2022**, *122*, 11675, https://doi.org/10.1021/acs.chemrev.2c00035.
[19] F. A. Plamper, W. Richtering, *Acc. Chem. Res.* **2017**, *50*, 131, https://doi.org/10.1021/acs.accounts.6b00544.
[20] H. Mehrabian, J. Harting, J. H. Snoeijer, *Soft Matter* **2016**, *12*, 1062, https://doi.org/10.1039/C5SM01971K.
[21] F. Camerin, N. Gnan, J. Ruiz-Franco, A. Ninarello, L. Rovigatti, E. Zaccarelli, *Phys. Rev. X* **2020**, *10*, 031012, https://doi.org/10.1103/PhysRevX.10.031012.
[22] J. Kolker, L. Fischer, A. M. Menzel, H. Löwen, *J. Elast.* **2022**, *150*, 77, https://doi.org/10.1007/s10659-022-09897-1.
[23] B. S. Murray, *Adv. Colloid Interface Sci.* **2019**, *271*, 101990, https://doi.org/10.1016/j.cis.2019.101990.
[24] N. Nussbaum, J. Bergfreund, J. Vialetto, L. Isa, P. Fischer, *Colloid Surf. B Biointerfaces* **2022**, *217*, 112595, https://doi.org/10.1016/j.colsurfb.2022.112595.
[25] W. Richtering, *Langmuir* **2012**, *28*, 17218, https://doi.org/10.1021/la302331s.
[26] B. M. Rey, R. Elnathan, R. Ditcovski, K. Geisel, M. Zanini, M.-A. Fernandez-Rodriguez, V. V. Naik, A. Frutiger, W. Richtering, T. Ellenbogen, N. H. Voelcker, L. Isa, *Nano Lett.* **2016**, *16*, 157, https://doi.org/10.1021/acs.nanolett.5b03414.
[27] J. Kim, S. Nayak, L. A. Lyon, *J. Am. Chem. Soc.* **2005**, *127*, 9588, https://doi.org/10.1021/ja0519076.
[28] S. Tsuji, H. Kawaguchi, *Langmuir* **2005**, *21*, 8439, https://doi.org/10.1021/la050271t.
[29] O. S. Deshmukh, A. Maestro, M. H. G. Duits, D. van den Ende, M. C. Stuart, F. Mugele, *Soft Matter* **2014**, *10*, 7045, https://doi.org/10.1039/C4SM00566J.

[30] L. Isa, E. Amstad, K. Schwenke, E. Del Gado, P. Ilg, M. Kröger, E. Reimhult, *Soft Matter* **2011**, *7*, 7663, https://doi.org/10.1039/c1sm05407d.
[31] J. Vialetto, M. Zanini, L. Isa, *Curr. Opin. Colloid Interface Sci*. **2022**, *58*, 101560, https://doi.org/10.1016/j.cocis.2021.101560.
[32] E. Guzmán, F. Martínez-Pedrero, C. Calero, A. Maestro, F. Ortega, R. G. Rubio, *Adv. Colloid Interface Sci*. **2022**, *302*, 102620, https://doi.org/10.1016/j.cis.2022.102620.
[33] A. Maestro, E. Guzmán, F. Ortega, R. G. Rubio, *Curr. Opin. Colloid Interface Sci*. **2014**, *19*, 355, https://doi.org/10.1016/j.cocis.2014.04.008.
[34] J. Menath, J. Eatson, R. Brilmayer, A. Andrieu-Brunsen, D. M. A. Buzza, N. Vogel, *Proc. Natl. Acad. Sci.* **2021**, *118*, e2113394118, https://doi.org/10.1073/pnas.2113394118.
[35] M. Rey, M. Á. Fernández-Rodríguez, M. Steinacher, L. Scheidegger, K. Geisel, W. Richtering, T. M. Squires, L. Isa, *Soft Matter* **2016**, *12*, 3545, https://doi.org/10.1039/C5SM03062E.
[36] J. Vialetto, F. Camerin, F. Grillo, S. N. Ramakrishna, L. Rovigatti, E. Zaccarelli, L. Isa, *ACS Nano* **2021**, *15*, 13105, https://doi.org/10.1021/acsnano.1c02486.
[37] T. Liu, S. Seiffert, J. Thiele, A. R. Abate, D. A. Weitz, W. Richtering, *Proc. Natl. Acad. Sci. USA* **2012**, *109*, 384, https://doi.org/10.1073/pnas.1019196109.
[38] S. Ciarella, M. Rey, J. Harrer, N. Holstein, M. Ickler, H. Löwen, N. Vogel, L. M. C. Janssen, *Langmuir* **2021**, *37*, 5364, https://doi.org/10.1021/acs.langmuir.1c00541.
[39] M. Destribats, V. Lapeyre, M. Wolfs, E. Sellier, F. Leal-Calderon, V. Ravaine, V. Schmitt, *Soft Matter* **2011**, *7*, 7689, https://doi.org/10.1039/c1sm05240c.
[40] K. Geisel, L. Isa, W. Richtering, *Langmuir* **2012**, *28*, 15770, https://doi.org/10.1021/la302974j.
[41] F. Camerin, M. Á. Fernández-Rodríguez, L. Rovigatti, M.-N. Antonopoulou, N. Gnan, A. Ninarello, L. Isa, E. Zaccarelli, *ACS Nano* **2019**, *13*, 4548, https://doi.org/10.1021/acsnano.9b00390.
[42] L. Costa, G. Li-Destri, N. H. Thomson, O. Konovalov, D. Pontoni, *Nano Lett*. **2016**, *16*, 5463, https://doi.org/10.1021/acs.nanolett.6b01877.
[43] Y. Chai, A. Lukito, Y. Jiang, P. D. Ashby, T. P. Russell, *Nano Lett.* **2017**, *17*, 6453, https://doi.org/10.1021/acs.nanolett.7b03462.
[44] L. Costa, G. Li-Destri, D. Pontoni, O. Konovalov, N. H. Thomson, *Adv. Mater. Interfaces* **2017**, *4*, 1700203, https://doi.org/10.1002/admi.201700203.
[45] P. Gu, Y. Chai, H. Hou, G. Xie, Y. Jiang, Q. Xu, F. Liu, P. D. Ashby, J. Lu, T. P. Russell, *Angew. Chemie Int. Ed*. **2019**, *58*, 12112, https://doi.org/10.1002/anie.201906339.
[46] Y. Chai, J. Hasnain, K. Bahl, M. Wong, D. Li, P. Geissler, P. Y. Kim, Y. Jiang, P. Gu, S. Li, D. Lei, B. A. Helms, T. P. Russell, P. D. Ashby, *Sci. Adv*. **2020**, *6*, 1, https://doi.org/10.1126/sciadv.abb8675.
[47] J. Vialetto, S. N. Ramakrishna, L. Isa, **2022**, http://arxiv.org/abs/2204.09324; J. Vialetto, S. N. Ramakrishna, L. Isa, *Sci. Adv.* **2022**, accepted.
[48] S. Bochenek, A. Scotti, W. Ogieglo, M. Á. Fernández-Rodríguez, M. F. Schulte, R. A. Gumerov, N. V. Bushuev, I. I. Potemkin, M. Wessling, L. Isa, W. Richtering, *Langmuir* **2019**, *35*, 16780, https://doi.org/10.1021/acs.langmuir.9b02498.
[49] K. Zielińska, H. Sun, R. A. Campbell, A. Zarbakhsh, M. Resmini, *Nanoscale* **2016**, 8, 4951, https://doi.org/10.1039/C5NR07538F.
[50] S. Bochenek, F. Camerin, E. Zaccarelli, A. Maestro, M. M. Schmidt, W. Richtering, A. Scotti, *Nat. Commun*. **2022**, *13*, 3744, https://doi.org/10.1038/s41467-022-31209-3.
[51] K. Horigome, D. Suzuki, *Langmuir* **2012**, *28*, 12962, https://doi.org/10.1021/la302465w.
[52] M. Kwok, T. Ngai, *J. Colloid Interface Sci*. **2016**, *461*, 409, https://doi.org/10.1016/j.jcis.2015.09.049.
[53] L. Hoppe Alvarez, A. A. Rudov, R. A. Gumerov, P. Lenssen, U. Simon, I. I. Potemkin, D. Wöll, *Phys. Chem. Chem. Phys*. **2021**, *23*, 4927, https://doi.org/10.1039/D0CP06355J.
[54] S. A. Vasudevan, A. Rauh, M. Kröger, M. Karg, L. Isa, *Langmuir* **2018**, *34*, 15370, https://doi.org/10.1021/acs.langmuir.8b03048.
[55] T. Hoare, D. McLean, *J. Phys. Chem. B* **2006**, *110*, 20327, https://doi.org/10.1021/jp0643451.
[56] M. Stieger, W. Richtering, J. S. Pedersen, P. Lindner, *J. Chem. Phys*. **2004**, *120*, 6197, https://doi.org/10.1063/1.1665752.
[57] I. Varga, T. Gilányi, R. Mészáros, G. Filipcsei, M. Zrínyi, *J. Phys. Chem. B* **2001**, *105*, 9071, https://doi.org/10.1021/jp004600w.
[58] D. Wilms, Y. Adler, F. Schröer, L. Bunnemann, S. Schmidt, *Soft Matter* **2021**, *17*, 5711, https://doi.org/10.1039/D1SM00291K.
[59] A. Mourran, Y. Wu, R. A. Gumerov, A. A. Rudov, I. I. Potemkin, A. Pich, M. Möller, *Langmuir* **2016**, *32*, 723, https://doi.org/10.1021/acs.langmuir.5b03931.
[60] A. Scotti, S. Bochenek, M. Brugnoni, M. A. Fernandez-Rodriguez, M. F. Schulte, J. E. Houston, A. P. H. Gelissen, I. I. Potemkin, L. Isa, W. Richtering, *Nat. Commun*. **2019**, *10*, 1418, https://doi.org/.1038/s41467-019-09227-5.
[61] A. Rauh, M. Rey, L. Barbera, M. Zanini, M. Karg, L. Isa, *Soft Matter* **2017**, *13*, 158, https://doi.org/10.1039/C6SM01020B.
[62] J. Harrer, M. Rey, S. Ciarella, H. Löwen, L. M. C. C. Janssen, N. Vogel, *Langmuir* **2019**, *35*, 10512, https://doi.org/10.1021/acs.langmuir.9b01208.
[63] A. Maestro, D. Jones, C. Sánchez de Rojas Candela, E. Guzman, M. H. G. G. Duits, P. Cicuta, *Langmuir* **2018**, *34*, 7067, https://doi.org/10.1021/acs.langmuir.7b03879.
[64] S. Bochenek, A. Scotti, W. Richtering, *Soft Matter* **2021**, *17*, 976, https://doi.org/10.1039/D0SM01774D.
[65] J. Vialetto, N. Nussbaum, J. Bergfreund, P. Fischer, L. Isa, *J. Colloid Interface Sci.* **2022**, *608*, 2584, https://doi.org/10.1016/j.jcis.2021.10.186.
[66] M. Destribats, V. Lapeyre, E. Sellier, F. Leal-Calderon, V. Schmitt, V. Ravaine, *Langmuir* **2011**, *27*, 14096, https://doi.org/10.1021/la203476h.
[67] R. W. Style, L. Isa, E. R. Dufresne, *Soft Matter* **2015**, *11*, 7412, https://doi.org/10.1039/C5SM01743B.
[68] L. Scheidegger, M. Á. Fernández-Rodríguez, K. Geisel, M. Zanini, R. Elnathan, W. Richtering, L. Isa, *Phys. Chem. Chem. Phys.* **2017**, *19*, 8671, https://doi.org/10.1039/C6CP07896F.
[69] C. Picard, P. Garrigue, M. C. Tatry, V. Lapeyre, S. Ravaine, V. Schmitt, V. Ravaine, *Langmuir* **2017**, *33*, 7968, https://doi.org/10.1021/acs.langmuir.7b01538.
[70] M. Ickler, J. Menath, L. Holstein, M. Rey, D. M. A. Buzza, N. Vogel, *Soft Matter* **2022**, *1*, 1, https://doi.org/10.1039/D2SM00644H.
[71] C. Monteux, C. Marlière, P. Paris, N. Pantoustier, N. Sanson, P. Perrin, *Langmuir* **2010**, *26*, 13839, https://doi.org/10.1021/la1019982.
[72] A. C. Nickel, A. Scotti, J. E. Houston, T. Ito, J. Crassous, J. S. Pedersen, W. Richtering, *Nano Lett.* **2019**, *19*, 8161, https://doi.org/10.1021/acs.nanolett.9b03507.
[73] A. C. Nickel, A. A. Rudov, I. I. Potemkin, J. J. Crassous, W. Richtering, *Langmuir* **2022**, *38*, 4351, https://doi.org/10.1021/acs.langmuir.2c00093.

License and Terms

The definitive version of this article is the electronic one that can be found at https://doi.org/10.2533/chimia.2022.852